JAERI-M
87-012

IMPROVEMENT OF ENERGY CONFINEMENT OF NEUTRAL BEAM HEATED PLASMA BY LOWER HYBRID CURRENT DRIVE IN JT-60

February 1987

Kenkichi USHIKUSA, Takeshi IMAI, Ryuji YOSHINO
Yoshitaka IKEDA, Keiji SAKAMOTO, Shinichi ISHIDA
Mamoru MATSUOKA and JT-60 Team

日本原子力研究所
Japan Atomic Energy Research Institute

JAERI-M レポートは，日本原子力研究所が不定期に公刊している研究報告書です。
入手の問合わせは，日本原子力研究所技術情報部情報資料課（〒319—11 茨城県那珂郡東海村）あて，お申しこしください。なお，このほかに財団法人原子力弘済会資料センター（〒319-11 茨城県那珂郡東海村日本原子力研究所内）で複写による実費頒布をおこなっております。

JAERI-M reports are issued irregularly.
Inquiries about availability of the reports should be addressed to Information Division, Department of Technical Information, Japan Atomic Energy Research Institute, Tokai-mura, Naka-gun, Ibaraki-ken 319-11, Japan.

編集兼発行　日本原子力研究所
印　　刷　山田軽印刷所

JAERI-M 87-012

Improvement of Energy Confinement of Neutral Beam Heated Plasma by Lower Hybrid Current Drive in JT-60

Kenkichi USHIGUSA, Takeshi IMAI, Ryuji YOSHINO
Yoshitaka IKEDA, Keiji SAKAMOTO, Shinichi ISHIDA
Mamoru MATSUOKA and JT-60 Team

Department of Large Tokamak Research
Naka Fusion Research Establishment
Japan Atomic Energy Research Institute
Naka-machi, Naka-gun, Ibaraki-ken

(Received January 26, 1987)

Energy and particle confinements in a high power neutral beam heated plasma are improved by a lower hybrid current drive (LHCD) in JT-60. A clear correlation between the improvement of the energy confinement time and the decrease of the plasma internal inductance caused by LHCD is observed. The energy confinement time of the profile-controlled plasma by LHCD is close to the ohmic confinement time and does not degrade with the beam absorption power up to 11 MW.

Keywords : Lower Hybrid Current Drive, Profile Control, Neutral Beam Heating, Improvement of Energy Confinement, JT-60

JT-60 Team

M.YOSHIKAWA, T.ABE, H.AKAOKA, H.AIKAWA, H.AKASAKA, M.AKIBA, N.AKINO, T.AKIYAMA, T.ANDO, K.ANNOH, N.AOYAGI, K.ARAKAWA, M.ARAKI, K.ARIMOTO, M.AZUMI, S.CHIBA, M.DAIRAKU, N.EBISWA, T.FUJII, T. FUKUDA, H.FURUKAWA, K.HAMAMATSU, K.HAYASHI, M.HARA, K.HARAGUCHI, H.HIRATSUKA, T.HIRAYAMA, S.HIROKI, K.HIRUTA, M.HONDA, H.HORIIKE, R.HOSODA, N.HOSOGANE, Y.IIDA, T.IIJIMA, K.IKEDA, Y.IKEDA, T.IMAI, T.INOUE,, N.ISAJI, M.ISAKA, S.ISHIDA, N.ITIGE, T.ITO, Y.ITO, A.KAMINAGA, M.KAWAI, Y.KAWAMATA, K.KAWASAKI, K.KIKUCHI, M.KIKUCHI, H.KIMURA, T.KIMURA, H.KISHIMOTO, K.KITAHARA, S.KITAMURA, A.KITSUNEZAKI, K.KIYONO, N.KOBAYASHI, K.KODAMA, Y.KOIDE, T.KOIKE, M.KOMATA, I.KONDO, S.KONOSHIMA, H.KUBO, S.KUNIEDA, S.KURAKATA, K.KURIHARA, M.KURIYAMA, T.KURODA, M.KUSAKA, Y.KUSAMA,, S.MAEHARA, K.MAENO, S.MATSUDA, S.MASE, M.MATSUKAWA, T.MATSUKAWA, M.MATSUOKA, N.MIYA, K.MIYATI, Y.MIYO, K.MIZUHASHI, M.MIZUNO, R.MURAI, Y.MURAKAMI, M.MUTO, M.NAGAMI, A.NAGASHIMA, K.NAGASHIMA, T.NAGASHIMA, S.NAGAYA, H.NAKAMURA, Y.NAKAMURA, M.NEMOTO, Y.NEYATANI, S.NIIKURA, H.NINOMIYA, T.NISHITANI, H.NOMATA, K.OBARA, N.OGIWARA, T.OHGA, Y.OHARA, K.OHASA, H.OHHARA, T.OHSHIMA, M.OHKUBO, K.OHTA, M.OHTA, M.OHTAKA, Y.OHUCHI, A.OIKAWA, H.OKUMURA, Y.OKUMURA, K.OMORI, S.OMORI, Y.OMORI, T.OZEKI, A.SAKASAI, S.SAKATA, M.SATOU, M.SAIGUSA, K.SAKAMOTO, M.SAWAHATA, M.SEIMIYA, M.SEKI, S.SEKI, K.SHIBANUMA, R.SHIMADA, K.SHIMIZU, M.SHIMIZU, Y.SHIMOMURA, S.SHINOZAKI, H.SHIRAI, H.SHIRAKATA, M.SHITOMI, K.SUGANUMA, T.SUGIE, T.SUGIYAMA, H.SUNAOSHI, K.SUZUKI, M.SUZUKI, M.SUZUKI, N.SUZUKI, S.SUZUKI, Y.SUZUKI, M.TAKAHASHI, S.TAKAHASHI, T.TAKAHASHI, H.TAKAHASHI*, M.TAKASAKI, M.TAKATSU, H.TAKEUCHI, A.TAKESHITA, S.TAMURA, S.TANAKA, K.TANI, M.TERAKADO, T.TERAKADO, K.TOBITA, T.TOKUTAKE, T.TOTSUKA, N.TOYOSHIMA, H.TSUDA, T.TSUGITA, S.TSUJI, Y.TSUKAHARA, M.TSUNEOKA, K.UEHARA, M.UMEHARA, Y.URAMOTO, H.USAMI, K.USHIGUSA, K.USUI, J.YAGYU, K.YAMADA, M.YAMAMOTO, O.YAMASHITA, Y.YAMASHITA, K.YANO, T.YASUKAWA, K.YOKOKURA, H.YOKOMIZO, H.YOSHIDA, Y.YOSHINARI, R.YOSHINO, I.YONEKAWA, K.WATANABE

JT－60におけるLH電流駆動によるNB加熱プラズマの閉じ込め特性の改善

日本原子力研究所那珂研究所臨界プラズマ研究部
牛草　健吉・今井　　剛・芳野　隆治
池田　佳隆・坂本　慶司・石田　真一
松岡　　守・JT－60チーム

（1987年1月26日受理）

JT－60における高入力のNB加熱プラズマのエネルギ及び粒子閉じ込め特性は，LHの電流駆動によって改善される。閉じ込め特性の改善とプラズマの内部インダクタンスの減少の間には明らかな相関関係が見られた。LH電流駆動による電流分布の制御が，NB加熱入力11 MWにおいても，プラズマの閉じ込め特性の劣化を防ぎ，ジュール・プラズマの閉じ込め特性と同程度の結果を与えている。

那珂研究所：〒311－02　茨城県那珂郡那珂町大字向山801－1

相川 裕史, 青柳 哲雄, 赤岡 伸雄, 赤坂 博美, 秋野 昇, 秋場 真人, 秋山 隆,
安積 正史, 阿部 哲也, 新井 貴, 荒川喜代次, 荒木 政則, 有本 公子, 安東 俊郎,
安納 勝人, 飯島 勉, 飯田 幸生, 池田 幸治, 池田 佳隆, 井坂 正義, 伊佐治信明,
石田 真一, 市毛 尚志, 伊藤 孝雄, 伊藤 康浩, 井上多加志, 今井 剛, 上原 和也,
宇佐美広次, 牛草 健吉, 薄井 勝富, 梅原 昌敏, 浦本 保幸, 海老沢 昇, 及川 晃,
大麻 和美, 大内 豊, 大賀 徳道, 大久保 実, 大島 貴幸, 太田 和也, 太田 充,
大高 光夫, 大原比呂志, 大森憲一郎, 大森 俊造, 大森 栄和, 荻原 徳男, 奥村 裕司,
奥村 義和, 小関 隆久, 小原建治郎, 小原 祥裕, 神永 敦嗣, 河合視己人, 川崎 幸三,
川俣 陽一, 菊池 勝美, 菊池 満, 岸本 浩, 北原 勝美, 北村 繁, 狐崎 晶雄,
木村 豊秋, 木村 晴行, 清野 公廣, 日下 誠, 草間 義紀, 国枝 俊介, 久保 博孝,
倉形 悟, 栗原 研一, 栗山 正明, 黒田 猛, 小池 常之, 小出 芳彦, 児玉 幸三,
木島 滋, 小林 則幸, 小又 将夫, 近藤 育朗, 三枝 幹雄, 逆井 章, 坂田 信也,
坂本 慶司, 佐藤 正泰, 沢畠 正之, 鄯 守正, 篠崎 信一, 柴沼 清, 嶋田 隆一,
清水 勝宏, 清水 正亜, 下村 安夫, 白井 浩, 白形 弘文, 菅沼 和明, 杉江 達夫,
杉山 隆, 鈴木 貞明, 鈴木 國弘, 鈴木 紀男, 鈴木 正信, 鈴木 道雄, 鈴木 康夫,
砂押 秀則, 清宮 宗孝, 関 省吾, 関 正美, 高崎 学, 高津 英幸, 高橋 春次,
高橋虎之助, 高橋 弘法, 高橋 実, 竹内 浩, 竹下 明, 田中 茂, 田中竹次郎,
谷 啓二, 田村 早苗, 大楽 正幸, 千葉 真一, 塚原 美光, 次田 友宣, 辻 俊二,
津田 文男, 恒岡まさき, 寺門 恒久, 寺門 正之, 徳竹 利国, 戸塚 俊之, 飛田 健次,
豊島 昇, 中村 博雄, 中村 幸治, 長島 章, 永島 圭介, 永島 孝, 永谷 進,
永見 正幸, 新倉 節夫, 西谷 健夫, 二宮 博正, 根本 正博, 闍谷 譲, 野亦 英幸,
濱松 清隆, 林 和夫, 原 誠, 原口 和三, 平塚 一, 平山 俊雄, 蛭田 和治,
広木 成治, 福田 武司, 藤井 常幸, 古川 弘, 細金 延幸, 細山隆一郎, 堀池 寛,
本田 正男, 前野 勝樹, 前原 直, 間瀬 修次, 松岡 守, 松川 達哉, 松川 誠,
松田慎三郎, 水野 誠, 水橋 清, 宮 直之, 宮地 謙吾, 三代 康彦, 武藤 貢,
村井 隆一, 村上 義夫, 柳生 純一, 安川 亨, 矢野 勝久, 山下 修, 山下 幸彦,
山田喜美雄, 山本 正弘, 横倉 賢治, 横溝 英明, 吉川 和伸, 吉川 允二, 吉田 英俊,
吉成 洋治, 芳野 隆治, 米川 出, 渡辺 和弘,

Contents

目　　次

1. Introduction

Sawteeth stabilization by the lower hybrid current drive (LHCD) have been reported in many tokamaks (PLT[1], ALCATOR-C[2], PETULA[3], ASDEX[4]). Stabilization of sawtooth oscilations leads to the increase of central electron temperature and consequently may improve the energy confinement time. The peaked temperature profile obtained by sawtooth stabilization has a quite different profile from that of usual OH plasmas and additionally heated plasmas[1]. These results indicate that LHCD can decouple the electron temperature profile from the current profile and may lead us to control the MHD stability and the energy confinement property. Recent experiment in ASDEX shows that stabilization of sawteeth in the neutral beam (NB) heated plasma by LHCD has improved the energy confinement time by a factor of 1.3 as compared with the case in the presence of sawteeth[5]. This improvement arises from the increase of the central electron temperature due to the sawteeth stabilization.

In this paper improvements of the energy and the particle confinement in the high power NB heated plasma by LHCD are reported. Experiments were carried out mainly with relatively high-q discharges ($q_{eff} \sim 5.5$) and only small volume where sawteeth dominate the energy loss exists within the plasma so that sawteeth does not largetly affect on the total energy content. Even in these conditions, LHCD has largely improved the energy confinement and a clear correlation between the deformation of current profile from OH plasma and the improvement of energy confinement has been observed. The global energy confinement time of the profile-controlled plasma stays near the Ohmic confinement time and does not degrade with the absorption power up to 11 MW.

JT-60 is a large tokamak with a poloidal divertor having a major radius of $R = 3.1$ m and a minor radius of $a_p = 0.9$ m[6]. Experiments presented in this paper were performed in the hydrogen or the helium plasma with the parameter range $\bar{n}_e = 0.2 - 1.6 \times 10^{19}$ m^{-3}, $I_p = 0.5 - 1.5$ MA, $B_T = 4$ T, $q_{eff} = 3.7 - 11$. In the helium discharges the hydrogen was always employed as the prefilling gas so that the helium plasma contains the hydrogen minority. The torus input power of RF up to 1.4 MW was injected from the 8×4 grill launcher at a frequency of 2 GHz. The power spectrum of the excited wave from this launcher peaks at the refractive index along the magnetic field $N_{/\!/} = 1.7$ with the width $\Delta N_{/\!/} \sim 1$ can be obtained by the toroidal phasing $\Delta\phi = 90°$. The hydrogen

NB[6] having the port-through power up to 20 MW with the beam energy of 40 - 70 keV was almost perpendiculally injected to the LHCD plasma. Relatively high current drive efficiency $\eta_{CD} \equiv \bar{n}_e(10^{19}m^{-3})R(m)I_{RF}(MA)/P_{LH}(MW) = 1 \sim 1.7$ for the Ohmic heated plasma and the improvement of drive efficiency by the combination with the NB heating ($\eta_{CD} = 2 - 3$) were successfully obtained in JT-60[7].

2. Improvement of the particle confinement time

In LHCD experiments on VERSATOR-II a significant density increase ($\Delta\bar{n}_e/n_e = 0.5 - 2$) and the improvement of the global particle confinement time ($\tau_p(\text{LHCD}) \sim 2.3\ \tau_p(\text{OH})$) have been observed[8]. In NB heated plasma, the global particle confinement time was investigated in JT-60. Figure 1 shows time evolutions of the electron density $\bar{n}_e$, $\beta_p + \ell_i/2$, port-through powers of NB and RF, the plasma current I_p and the loop voltage V_ℓ for the combination of NB and LHCD (solid lines) and for the NB heating into the OH plasma (broken lines). The bottom box of this figure is density profiles at t = 6 sec. After the onset of LH pulse at t ~ 3 sec, the loop voltage V_ℓ becomes negative value and the plasma current I_p = 0.7 MA is completely replaced to the RF current. The slow decrease with the time constant of several seconds in $\beta_p + \ell_i/2$ during the LH pulse shows the broader current profile was realized by LHCD than by the OH discharge. Under these conditions, the significant density increase form 0.33×10^{19} m^{-3} to 1.15×10^{19} m^{-3} was observed during the additional NB pulse. On the other hand, the NB heating into the OH plasma shows a modest increase from 0.33×10^{19} m^{-3} to 0.55×10^{19} m^{-3}. The density increase of the combined NB heating with LHCD was always larger than that of the other. A comparision between both density profiles at t = 6 sec as shown in the bottom box of this figure indicates that the more peaked density profile is formed for the combination of NB and LHCD. The sharp density profile may mean that the particle diffusion is suppressed in the core region of the plasma. The above results suggest that the particle confinement in the NB heated plasma can be improved by LHCD.

Figure 2 shows the density dependence of the global particle confinement time τ_p for OH plasmas (open notations) and NB heated (closed notations) where the particle confinement time is calculated

NB[6] having the port-through power up to 20 MW with the beam energy of 40 - 70 keV was almost perpendiculally injected to the LHCD plasma. Relatively high current drive efficiency $\eta_{CD} \equiv \bar{n}_e(10^{19}m^{-3})R(m)I_{RF}(MA)/P_{LH}(MW) = 1 \sim 1.7$ for the Ohmic heated plasma and the improvement of drive efficiency by the combination with the NB heating ($\eta_{CD} = 2 - 3$) were successfully obtained in JT-60[7].

2. Improvement of the particle confinement time

In LHCD experiments on VERSATOR-II a significant density increase ($\Delta\bar{n}_e/n_e = 0.5 - 2$) and the improvement of the global particle confinement time ($\tau_p(\text{LHCD}) \sim 2.3\ \tau_p(\text{OH})$) have been observed[8]. In NB heated plasma, the global particle confinement time was investigated in JT-60. Figure 1 shows time evolutions of the electron density $\bar{n}_e$, $\beta_p + \ell_i/2$, port-through powers of NB and RF, the plasma current I_p and the loop voltage V_ℓ for the combination of NB and LHCD (solid lines) and for the NB heating into the OH plasma (broken lines). The bottom box of this figure is density profiles at t = 6 sec. After the onset of LH pulse at t ~ 3 sec, the loop voltage V_ℓ becomes negative value and the plasma current $I_p = 0.7$ MA is completely replaced to the RF current. The slow decrease with the time constant of several seconds in $\beta_p + \ell_i/2$ during the LH pulse shows the broader current profile was realized by LHCD than by the OH discharge. Under these conditions, the significant density increase form 0.33×10^{19} m^{-3} to 1.15×10^{19} m^{-3} was observed during the additional NB pulse. On the other hand, the NB heating into the OH plasma shows a modest increase from 0.33×10^{19} m^{-3} to 0.55×10^{19} m^{-3}. The density increase of the combined NB heating with LHCD was always larger than that of the other. A comparision between both density profiles at t = 6 sec as shown in the bottom box of this figure indicates that the more peaked density profile is formed for the combination of NB and LHCD. The sharp density profile may mean that the particle diffusion is suppressed in the core region of the plasma. The above results suggest that the particle confinement in the NB heated plasma can be improved by LHCD.

Figure 2 shows the density dependence of the global particle confinement time τ_p for OH plasmas (open notations) and NB heated (closed notations) where the particle confinement time is calculated

by using the global particle balance equation with the H_α radiation profile[9]. The particle confinement time in the NB heated plasma is shorter than that of the Ohmic plasma by a factor of about 2. The particle confinement time in the combination of NB heating and LHCD is plotted by an asterisk(*) this value is higher than that of the usual beam heating by a factor of about 1.3. We can say that the global particle confinement time in the NB heated plasma is improved by the LHCD.

3. Improvement of the energy confinement

The combined NB heating experiments with LHCD were carried out in relatively low density regime because the injected power of RF was not high enough to drive RF current in the high density plasma. Therefore the temperature measurement using the Thomson scattering was not available in these experiments and only the magnetic measurement to identify the incremental stored energy was employed here.

Figure 3 shows time evolutions of the loop voltage V_ℓ, the Shafranov lamda $\Lambda \equiv \beta_p + \ell_i/2 - 1$ and the line integrated electron density $\bar{n}_e\ell$ for the NB heating into the OH plasma (a), and the combined NB and LH (b) and (c). In the case (a), the NB power with the beam energy of 40 keV was injected to the helium discharge having the average electron density of 0.2×10^{19} m^{-3}. An increase of the stored energy ΔW^* is 0.21 MJ with the beam absorption power of 3.4 MW and then the incremental energy confinement time[10] $\tau_E^{INC} \equiv \Delta W^*/P_{abs}$ of 62 msec is obtained. In the case (b), two RF pulses were applied to the almost the same condition with the case (a). As switched on at t = 3 sec with the pulse length Δt_{RF} = 0.5 sec, the first pulse is not seen in this figure. The second pulse was applied at t ~ 4 sec about 1 sec before the NB pulse. During the RF pulse the plasma current I_p of 1 MA is replaced by the RF current as shown in the loop voltage. After a rapid increase of $\Lambda \equiv \beta_p + \ell_i/2 - 1$ at the initial stage of RF pulse, it decrease slowly with the time constant of several seconds. The change of Λ in this period can be interpreted as being mainly due to the change of the plasma internal inductance ℓ_i. While the rapid rise of Λ contains the increase of the poloidal beta value β_p due to the formation of the electron tail, this rise cannot be explained by the increase of β_p alone. These changes

by using the global particle balance equation with the H_α radiation profile[9]. The particle confinement time in the NB heated plasma is shorter than that of the Ohmic plasma by a factor of about 2. The particle confinement time in the combination of NB heating and LHCD is plotted by an asterisk(*) this value is higher than that of the usual beam heating by a factor of about 1.3. We can say that the global particle confinement time in the NB heated plasma is improved by the LHCD.

3. Improvement of the energy confinement

The combined NB heating experiments with LHCD were carried out in relatively low density regime because the injected power of RF was not high enough to drive RF current in the high density plasma. Therefore the temperature measurement using the Thomson scattering was not available in these experiments and only the magnetic measurement to identify the incremental stored energy was employed here.

Figure 3 shows time evolutions of the loop voltage V_ℓ, the Shafranov lamda $\Lambda \equiv \beta_p + \ell_i/2 - 1$ and the line integrated electron density $\bar{n}_e\ell$ for the NB heating into the OH plasma (a), and the combined NB and LH (b) and (c). In the case (a), the NB power with the beam energy of 40 keV was injected to the helium discharge having the average electron density of 0.2×10^{19} m^{-3}. An increase of the stored energy ΔW^* is 0.21 MJ with the beam absorption power of 3.4 MW and then the incremental energy confinement time[10] $\tau_E^{INC} \equiv \Delta W^*/P_{abs}$ of 62 msec is obtained. In the case (b), two RF pulses were applied to the almost the same condition with the case (a). As switched on at t = 3 sec with the pulse length Δt_{RF} = 0.5 sec, the first pulse is not seen in this figure. The second pulse was applied at t ~ 4 sec about 1 sec before the NB pulse. During the RF pulse the plasma current I_p of 1 MA is replaced by the RF current as shown in the loop voltage. After a rapid increase of $\Lambda \equiv \beta_p + \ell_i/2 - 1$ at the initial stage of RF pulse, it decrease slowly with the time constant of several seconds. The change of Λ in this period can be interpreted as being mainly due to the change of the plasma internal inductance ℓ_i. While the rapid rise of Λ contains the increase of the poloidal beta value β_p due to the formation of the electron tail, this rise cannot be explained by the increase of β_p alone. These changes

in the internal inductance ℓ_i during LHCD are explained in the appendix by using the equation of the magnetic field diffusion. We can infer that the broad current profile as compared with the case (a) are realized before the injection of NB. Under these conditions the effective absorption power $P_{abs} - \dot{W}$ of 4.6 MW leads to the increase of the stored energy of 0.4 MJ and the corresponding incremental energy confinement time is around 87 msec. Clear improvement on the incremental energy confinement time is observed in the combination of NB heating and LHCD. The case of a high power NB heating of the LHCD plasma is shown in the figure of (c). In order to avoid a large shine through of the NB the electron density is increased by the short gas puffing before the NB pulse. The increase of stored energy ΔW^*=0.96 MJ with the effective absorption power of 10.7 MW and the incremental confinement time τ_E^{INC} = 90 msec are obtained. The energy confinement is improved by LHCD even in the high power NB heating. It is important to note the fact that τ_E^{INC} for the case (c) where the strong gas puffing before the NB pulse was employed is almost the same value for the case (b). This implies that the time constant of the change of current profile in the core plasma where the global energy confinement is determined is so long that the short gas pulse does not affect the current profile. This tact is supported by MHD activities as mentioned later. We can say that the change of the internal inductance ℓ_i during the NB pulse is relatively small for a large change of $\Lambda \equiv \beta_p + \ell_i/2 - 1$ as shown in Fig. 3(c).

The global energy confinement time τ_E is determined as

$$\tau_E \equiv \frac{W_{OH} + W_{LH} + \Delta W^*}{P_{OH} + P_{abs}^{LH} + P_{abs}} \qquad (1)$$

where W_{OH}, W_{LH}, ΔW^* are the Ohmic stored energy, the increases of stored energy by RF power and the NB power, and P_{OH}, P_{abs}^{LH}, P_{abs} are the Ohmic input power, absorption powers of LH and NB. We cannot identify W_{OH}, ΔW_{LH} and P_{abs}^{LH} accurately from the magnetic measurement. In order to estimate roughly the global energy confinement time, we neglect ΔW_{LH} and P_{abs}^{LH} in eq. (1) and determine W_{OH} from the scaling law for the OH plasma in JT-60; $W_{OH}(MJ) = 0.157\ I_p(MA)^{0.86}\ \bar{n}_e(10^{19}m^{-3})^{0.62}$ (11). These assumptions are valid when the beam power is high enough to set $P_{abs} >> P_{abs}^{LH}$, P_{OH} and $W^* << \Delta W_{LH}$, W_{OH} as this experiment. Figure 4 shows the density

dependence of τ_E for the absorption power of NB is 11 MW and $I_p = 1.0$ MA. The energy confinement time of the normal NB heating and the combined NB heating with LHCD are plotted as open and closed circles, respectively. The Ohmic confinement time for $\bar{n}_e < 2 \times 10^{19}$ m^{-3}, $I_p = 1.0$ MA stays between two solid lines. Broken line is the τ_E calculated by the Kaye-Goldston scaling[12]. We can see that the global energy confinement time for the combined NB heating with LHCD is rather near the Ohmic confinement time. Global energy confinement times for the case of Fig. 3(a), (b) and (c) are estimated roughly to $\tau_E \sim 69$ msec, 100 msec and 107 msec, respectively. Thus the global confinement time τ_E in the combined heating does not degrade with the absorption power up to 11 MW which is almost the maximum absorption power of JT-60 NB heating in this density regime.

Figure 5 shows the dependence of the increase of stored energy ΔW^* on the effective absorption power $P_{abs} - \dot{W}$ for the NB heating into the OH plasma (open symbols) and for the combined NB heating with LHCD (closed symbols). The maximum incremental energy confinement time for the NB heating alone is around 70 msec while 90 msec for the combined heating. It is interesting that the improvement of the confinement time is not always realized by the combination of NB and LHCD. The confinement time τ_E^{INC} for the LH + NB shot without the improvement stays in the usual NB heating level. We found that the change of the current profile due to LHCD is the key parameter to improve the energy confinement. This fact is shown in Fig. 6(a) where the horizontal axis is the change of the $\Lambda \equiv \beta_p + \ell_i/2 - 1$ due to LHCD during the time interval from the applications of RF pulse to the beam injection, that is,

$$\Delta\Lambda_{LH} \equiv \Delta(\beta_p + \ell_i/2 - 1)$$

$$\equiv \Lambda(\text{just before NB pulse}) - \Lambda(\text{just before LH pulse}) \qquad (2)$$

and the vertical axis is τ_E^{INC}. The increase of β_p due to the formation of the electron tail can be estimated roughly by assuming that the monochromatic electron beam having the energy corresponding to $N_{/\!/} = 1.7$ carry the total RF current. Since $\Delta\beta_p \sim 0.01$ is deduced for $I_p = I_{RF} = 1$ MA from this estimation, we can put approximately $\Delta\Lambda_{LH} \sim \Delta(\ell_i/2)$. As shown in this figure the improvement of the energy confinement is attained when the broader current profile is realized by LHCD than by

the OH discharge. The incremental energy confinement times in the combined heating are plotted as a function of $\beta_p + \ell_i/2$ just before the NB pulse in Fig. 6(b) for the case of $I_p = 1$ MA. Since the poloidal beta β_p is small before the NB onset ($\beta_p << \ell_i$), the horizontal axis can be regarded approximately as $\ell_i/2$. Apparently broad current profile obtained by LHCD leads to the improvement of energy confinement. In the NB heating into the OH plasma, the energy confinement time did not depend strongly on the safety factor q_{eff} and the NB heating in the ramp up phase of the plasma current did not tend to improve the confinement time[13]. Therefore we can say that the broad current profile obtained by LHCD do improve the confinement time.

According to the change of the current profile by LHCD, MHD activitives are changed in the beam heated plasma. Since discharges discussed in this paper are relatively high q discharge ($q_{eff} \sim 5.5$ for $I_p = 1$ MA, $B_T = 4$ T) and low density, large sawteeth were not observed in the NB heating into the OH plasma. Therefore the stabilization of sawteeth does not increase largely the total energy content. Figure 7 shows comparision of MHD activities inside the plasma of the usual NB heating (a), (b) and the combined heating (c), (d). The left hand side of this figure indicates time evolutions of the soft X-ray signals S_x from the near center of plasma and the right side is radial profiles of the fluctuation level of soft X-ray $\Delta S_x/S_x$. In the usual NB heating as shown in Fig. 7(a), (b), strong MHD oscillations localized sharply near the plasma center have been observed at about the end of NB pulse. Fluctuation level reaches about 40 %. This oscillation is thought to be mainly the m=1 oscillation with a frequency of a few kHz and the safety factor at the magnetic axis supposed to be below unity. These MHD oscillations near the plasma center are dramatically suppressed in the combined NB heating with LHCD as shown in Fig. 7(c)(d). MHD oscillations having $\Delta S_x/S_x \sim 0.1$ have been found near the half radius. These results imply that the current profile is rearranged by LHCD so that the central q-value increases and the sharp on the current profile shifts to the outer region of plasma. This deduction is supported by the change of $\beta_p + \ell_i/2$-1 during the LH pulse. A candidate of the possible explanations of the improvement of the energy confinement by LHCD is the stabilization effect of these strong MHD oscillations in the center of the plasma. We can also deduce that the stabilization of these fluctuations may result from the reamangement of current profile

and the improvement of energy confinement may derive from the other mechanism.

Finally Fig. 8 shows the relation between $\Delta\Lambda_{LH}$ defined as eq.(2) and the RF power normalized by the electron density and the plasma current $P_{LH}/\bar{n}_e I_p$. The horizontal axis is proportional to I_{RF}/I_p. As shown in this figure, active control of the current profile by the input RF power and the electron density are possible. In other words we can externally control the energy confinement time in the NB heated plasma. Other parameter dependences of $\Delta\Lambda_{LH}$ such as the electron temperature and the launcher phasing and so on have been not studied for the restriction of the machine time in this series of experiments yet.

4. Conclusions and Discussions

We conclude in our experimental results as following way,

(1) LHCD has improved the global particle confinement time in the NB heated plasma by a factor of around 1.3.

(2) The energy confinement time in the NB heated plasma has been improved by LHCD and apparent correlation between the improvement of confinement and the change of the internal inductance caused by LHCD has been observed. In the profile-controlled plasma by LHCD The incremental energy confinement time τ_E^{INC} has been improved by a factor of 1.3 - 1.8 as compared with that of NB heating alone.

(3) The global energy confinement time τ_E of well-controlled plasma by LHCD has been close to the Ohmic level and did not degrade with the absorption power up to 11 MW.

Combined NB heating to the profile-controlled plasma by LHCD seems a possible method to realize the break-even condition in JT-60. For this goal we need to control the current profile in a higher plasma current $I_p \gtrsim 2$ MA and in a higher electron density $\bar{n}_e \gtrsim 2 \times 10^{19}$ m^{-3}. These experiments were not studied in this series of experiment because there was not enough time for the launcher aging. IN JT-60, individually controllable 3 units of LH system have a total generator power of 24 MW, and a next torus power of around 15 MW with a pulse duration of 10 sec at frequency from 1.7 GHz to 2.3 GHz. Therefore we can examine the way to approach the break-even condition by the combination of profile control of LHCD and the high power NB heating. After the broad current

and the improvement of energy confinement may derive from the other mechanism.

Finally Fig. 8 shows the relation between $\Delta\Lambda_{LH}$ defined as eq.(2) and the RF power normalized by the electron density and the plasma current $P_{LH}/\bar{n}_e I_p$. The horizontal axis is proportional to I_{RF}/I_p. As shown in this figure, active control of the current profile by the input RF power and the electron density are possible. In other words we can externally control the energy confinement time in the NB heated plasma. Other parameter dependences of $\Delta\Lambda_{LH}$ such as the electron temperature and the launcher phasing and so on have been not studied for the restriction of the machine time in this series of experiments yet.

4. Conclusions and Discussions

We conclude in our experimental results as following way,

(1) LHCD has improved the global particle confinement time in the NB heated plasma by a factor of around 1.3.

(2) The energy confinement time in the NB heated plasma has been improved by LHCD and apparent correlation between the improvement of confinement and the change of the internal inductance caused by LHCD has been observed. In the profile-controlled plasma by LHCD The incremental energy confinement time τ_E^{INC} has been improved by a factor of 1.3 - 1.8 as compared with that of NB heating alone.

(3) The global energy confinement time τ_E of well-controlled plasma by LHCD has been close to the Ohmic level and did not degrade with the absorption power up to 11 MW.

Combined NB heating to the profile-controlled plasma by LHCD seems a possible method to realize the break-even condition in JT-60. For this goal we need to control the current profile in a higher plasma current $I_p \gtrsim 2$ MA and in a higher electron density $\bar{n}_e \gtrsim 2 \times 10^{19}$ m^{-3}. These experiments were not studied in this series of experiment because there was not enough time for the launcher aging. IN JT-60, individually controllable 3 units of LH system have a total generator power of 24 MW, and a next torus power of around 15 MW with a pulse duration of 10 sec at frequency from 1.7 GHz to 2.3 GHz. Therefore we can examine the way to approach the break-even condition by the combination of profile control of LHCD and the high power NB heating. After the broad current

profile is realized by LHCD at the density lower than the density limit of LHCD (this limit of 2 GHz may be around 3×10^{19} m^{-3} for the hydrogen and $\gtrsim 4 \times 10^{19}$ m^{-3} for the helium), we can approach to the goal by the combination of the short gas puffing and the NB heating as employed in Fig. 3(c).

Acknowledgements

Authors would like to acknowledge the effort of the whole co-workers in JT-60 and in particular of the technical staffs of RF division. We also wish to express our thank to Drs. S. Mori, Y. Iso, and K. Tomabechi for their encouragements and supports.

profile is realized by LHCD at the density lower than the density limit of LHCD (this limit of 2 GHz may be around 3×10^{19} m^{-3} for the hydrogen and $\gtrsim 4 \times 10^{19}$ m^{-3} for the helium), we can approach to the goal by the combination of the short gas puffing and the NB heating as employed in Fig. 3(c).

Acknowledgements

Authors would like to acknowledge the effort of the whole co-workers in JT-60 and in particular of the technical staffs of RF division. We also wish to express our thank to Drs. S. Mori, Y. Iso, and K. Tomabechi for their encouragements and supports.

References

(1) S. Bernabei, R. Bell, A. Cavallo et al., in Proc. of 11th International Conference on Plasma Physics and Controlled Nucl. Fusion Research, Kyoto, 1986, IAEA-CN-4/F-II-1.

(2) M. Prokolab, P. Bonoli, K.I. Chen et al., in Proc. of 11th International Conference on Plasma Physics and Controlled Nucl. Fusion Research, Kyoto, 1986, IAEA-CN-4/F-II-2, S. Knowtton, M. Porkolab, Y. Takase et al., Phys. Rev. Lett., 57(1986)587.

(3) F. Parlange, G. Agarici, P. Blanc, et al., in Proc. of 12th European Conference on Controlled Fusion and Plasma Physics, Budapest, 1985, Vol. 2, p.172.

(4) F.X. Boldner, D. Eckhartt, F. Leuterer et al., in Proc. 13th European Conference on Controlled Fusion and Plasma Physics, Schliersee, 1986, Vol. II, p.343.

(5) F.X. Soldner, K. McCormic, D. Eckhartt et al., Phys. Rev. Lett., 57(1986)1137.

(6) JT-60 Team, Plasma Physics and Controlled Fusion 28(1986)1377.

(7) JT-60 Team, in Proc. of 11th International Conference on Plasma Physics and Controlled Nucl. Fusion Research, Kyoto, 1986, IAEA-CN-47/K-I-2.

(8) M. Porkolab, B. Blackwell, P. Bonoli, et al., in Proc. of 10th International Conference of Plasma Physics and Controlled Nuclear Fusion Research, 1984, IAEA-CN-44/F-II-1.

(9) K. Yamada et al., to be submitted in Nucl. Fusion.

(10) Y. Shimomura, K. Odajima, Report of Japan Atomic Energy Research Institute, JAERI-M 86-128.

(11) M. Kikuchi, T. Hirayama, K. Shimizu et al., Report of Japan Atomic Energy Research Institute, JAERI-M 87-008.

(12) S.M. Kaye, R.J. Goldston, Nucl. Fusion 25(1985)65.

(13) JT-60 Team, in Proc. of 11th International Conference on Plasma Physics and Controlled Nucl. Fusion Research, Kyoto, 1986, IAEA-CU-47/A-II-2.

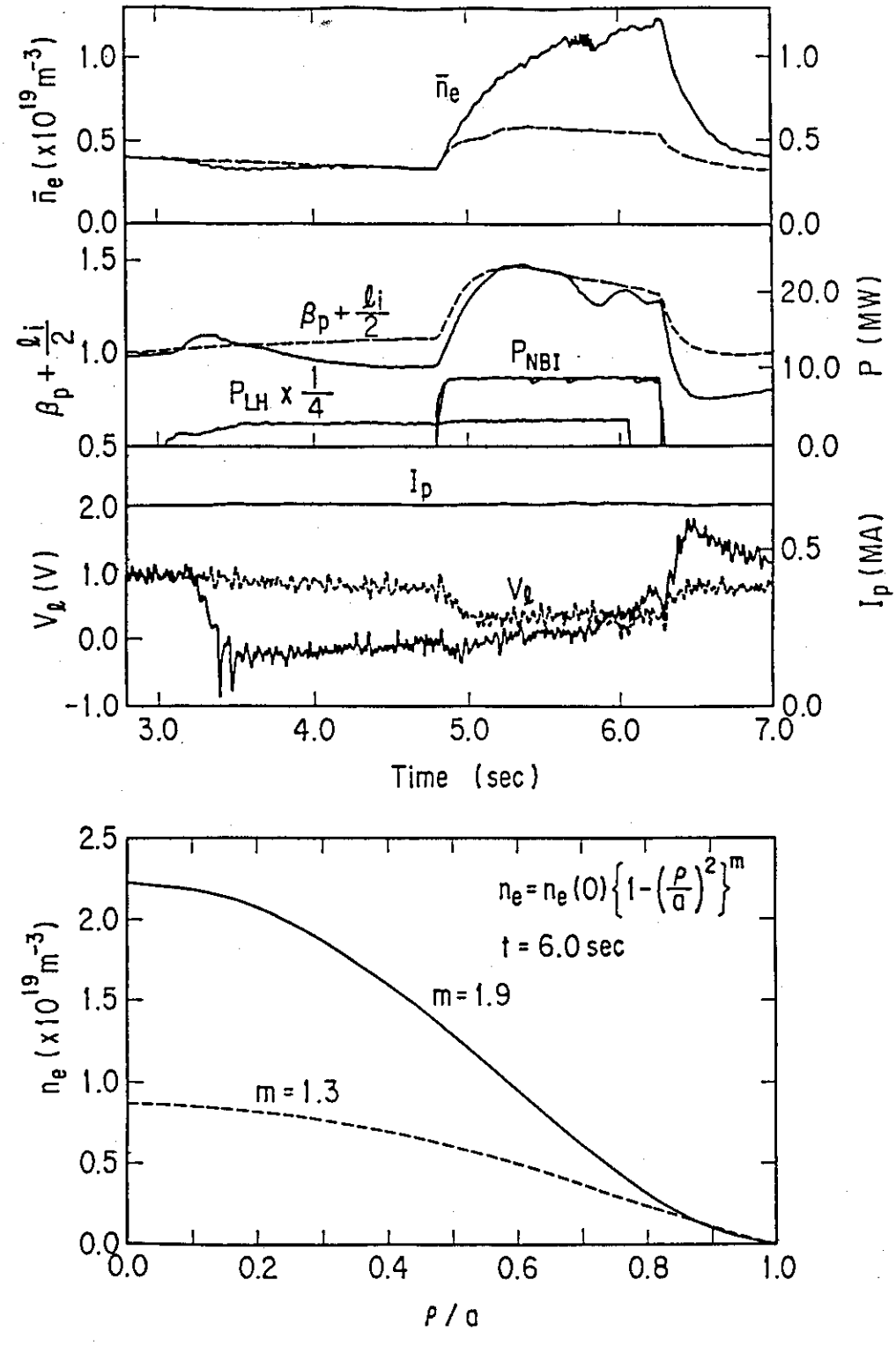

Fig. 1 Time evolutions of the electron density $\bar{n}_e$, $\beta_p + \ell_i/2$, the loop voltage V_ℓ and the density profile at t = 6 sec for the combined NB heating with LHCD (solid lines) and for the usual NB heating (broken lines). B_T = 4 T, I_p = 0.7 MA, H_e discharge and the beam energy V_{acc} = 40 keV.

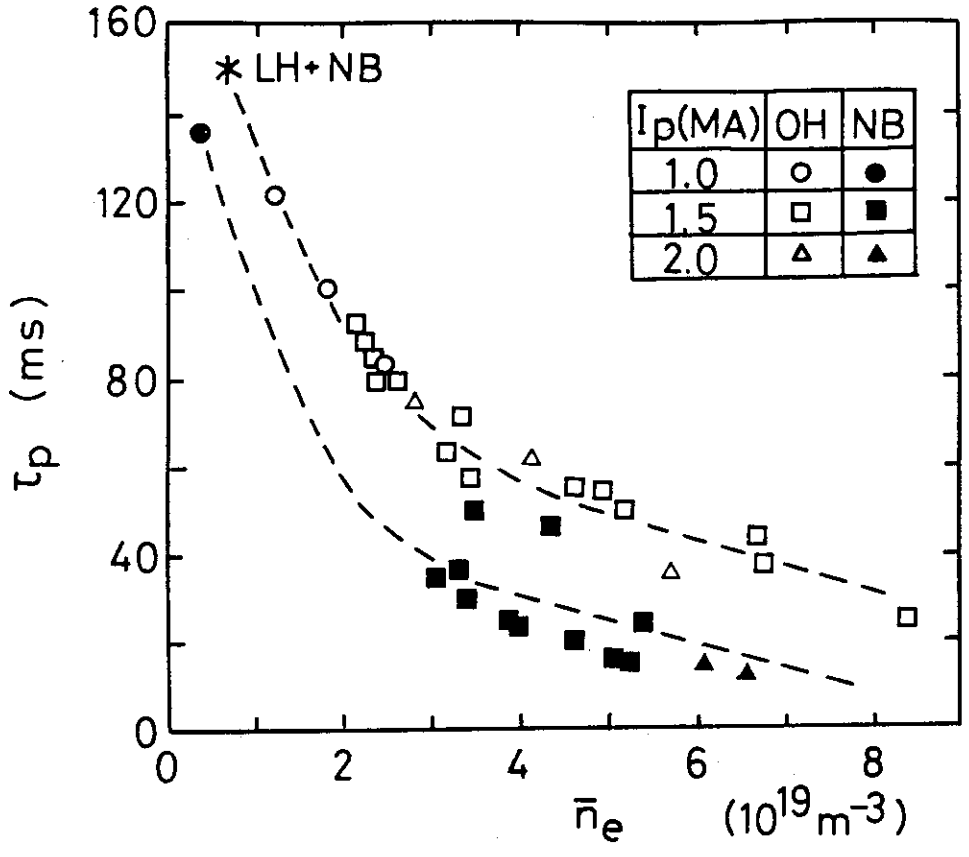

Fig. 2 Density dependence of the global particle confinement time τ_p for the Ohmic plasmas (open symbols) and the usual NB heated plasma (closed symbols). An asterisk(*) indicates the shot of the combined NB heating with LHCD (I_p = 1 MA, B_T = 4 T, H_e discharge, P_{LH} = 1.1 MW).

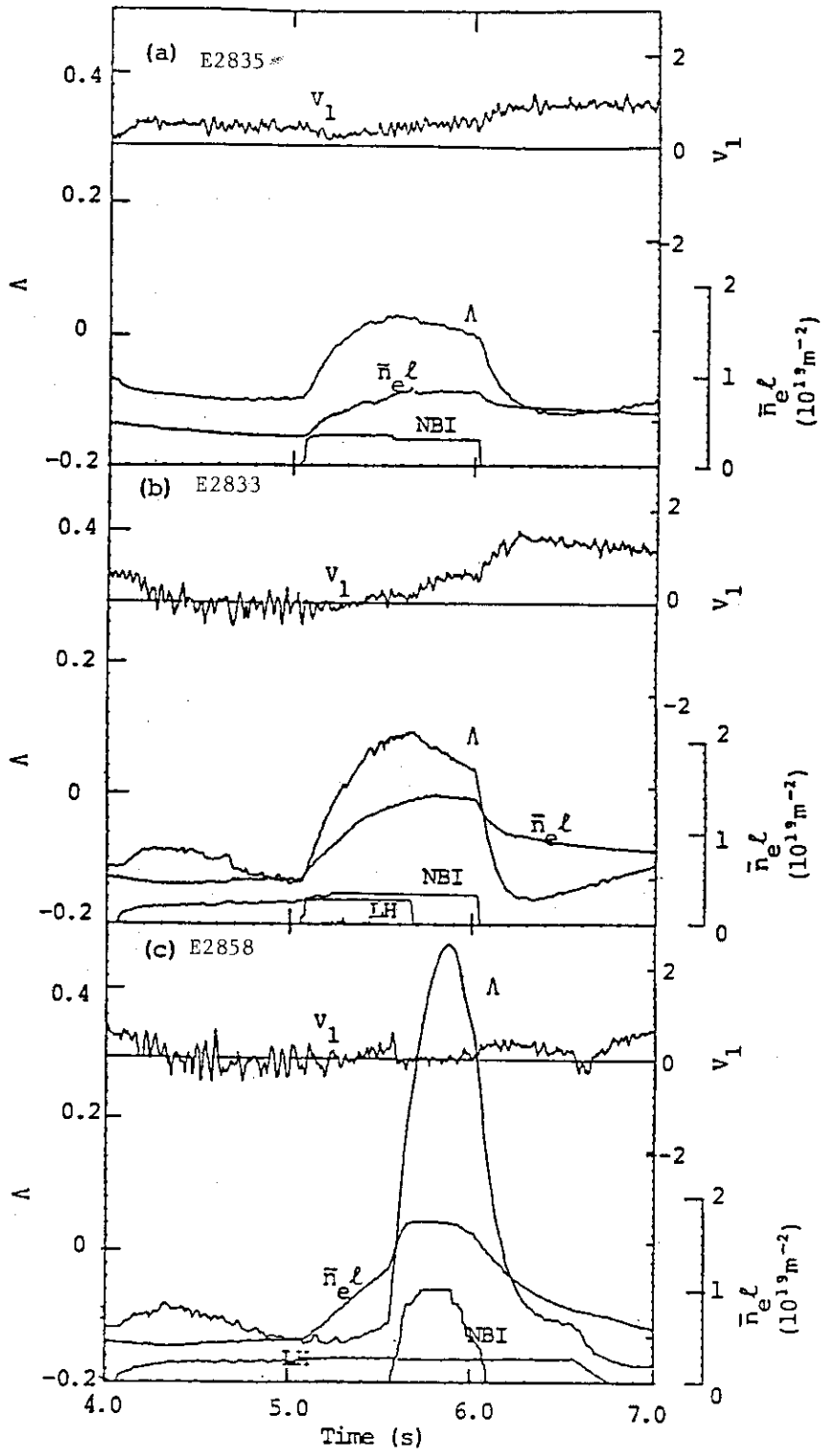

Fig. 3 The improvement of the energy confinement time. (a) shows the usual NB heating with V_{acc} = 40 keV, P_{abs} = 3.4 MW, ΔW^* = 0.207 MJ, τ_E^{INC} = 61 msec, (b) is the combined heating with V_{acc} = 40 keV, P_{abs} = 4.4 MW, P_{LH} = 1.1 MW, ΔW^* = 0.315 MJ, τ_E^{INC} = 71 msec. (c) shows the high power combined heating with V_{acc} = 70 keV, P_{abs} = 10.7 MW, P_{LH} = 1.1 MW, ΔW^* = 0.96 MJ, τ_E^{INC} = 90 msec. B_T = 4 T, I_p = 1 MA, H_e plasma and $\Lambda \equiv \beta_p + \ell_i/2-1$.

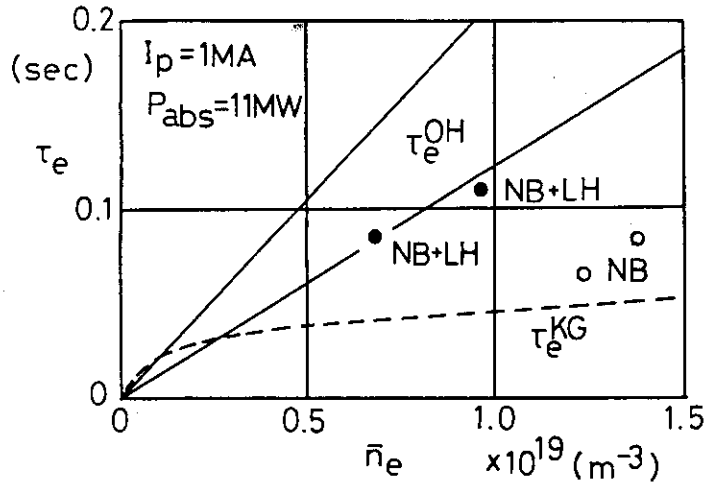

Fig. 4 Density dependence of the global energy confinement time τ_E for the combined NB heating with LHCD (●) and for the NB heating alone (○). The Ohmic confinement time for $\bar{n}_e < 2 \times 10^{19}$ m^{-3}, I_p = 1 MA stays inside two solid lines and the broken line is the τ_E calculated by the Kaye-Goldstore scaling law. I_p = 1 MA, B_T = 4 T.

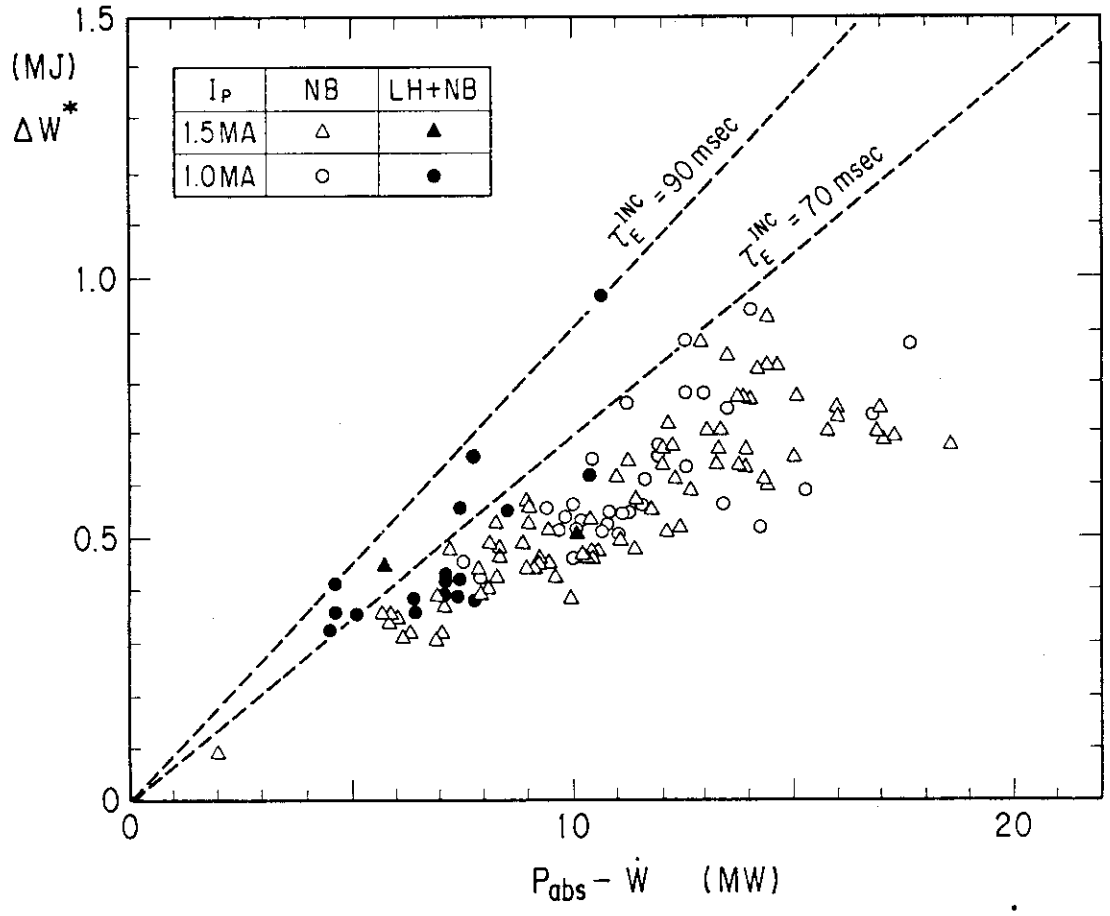

Fig. 5 The increase of the stored energy W* against $P_{abs} - \dot{W}$. Open symbols (○ , △) show the data of the usual NB heating and closed symbols (● , ▲) is the combined NB heating with LHCD.

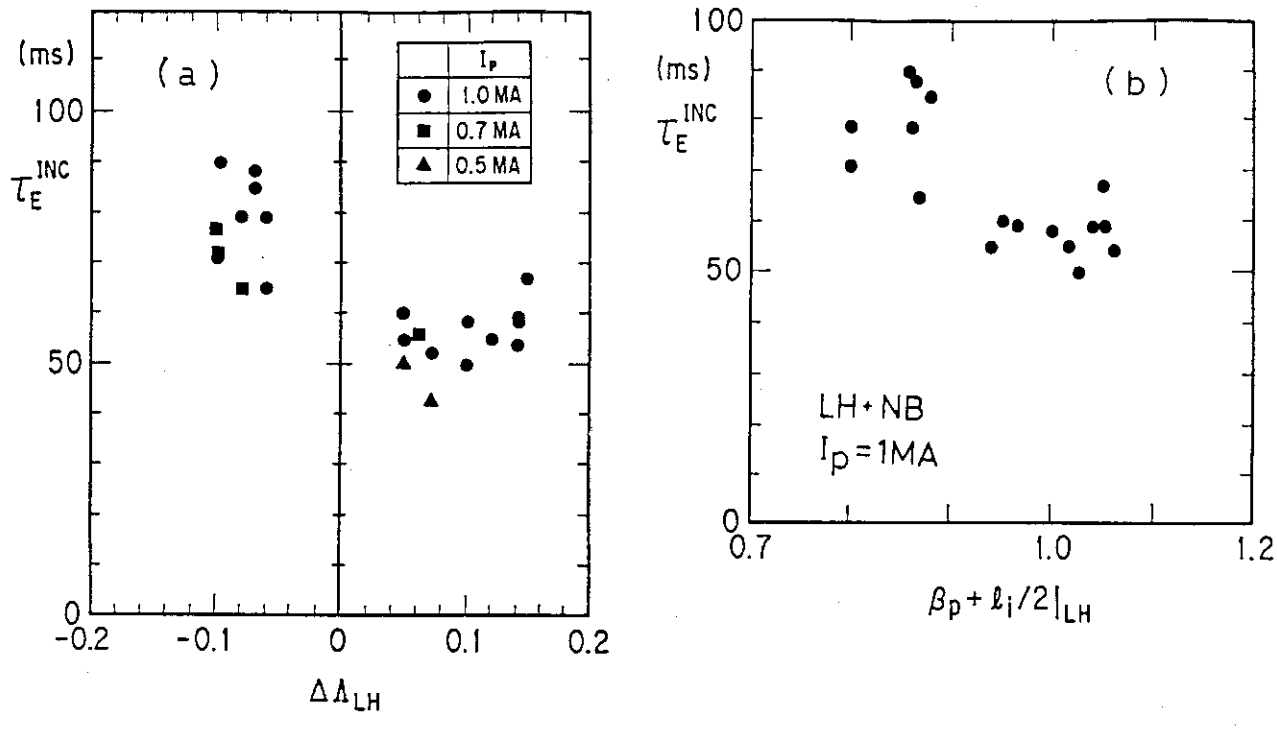

Fig. 6 (a) is the dependence of the incremental energy confinement time τ_E^{INE} on the change of $\Lambda = \beta_p + \ell_i/2-1$ due to LHCD $\Delta\Lambda_{LH}$ defined in eq.(2) and (b) is the τ_E^{INC} against $\beta_p + \ell_i/2$ just before the NB injection for $I_p = 1$ MA.

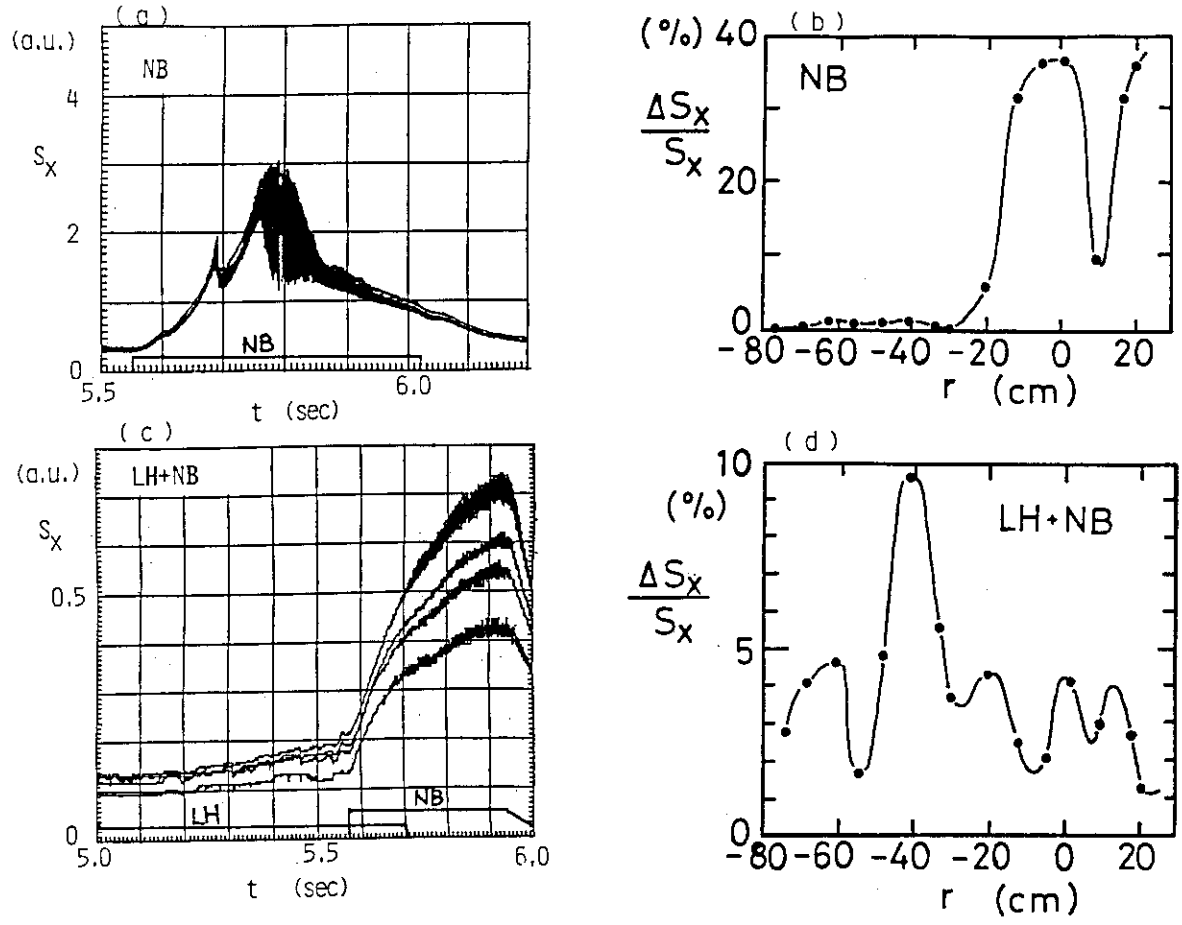

Fig. 7 Comparisions of the MHD activity of the usual NB heating (upper traces) and of the combined heating (lower traces). The left hand side of this figure shows time evolutions of the soft x-ray emission S_x from the near center chords and the right side is radial profiles of the fluctuation $\Delta S_x/S_x$. I_p = 1 MA, B_T = 4 T, $\bar{n}_e = 0.7 \times 10^{19}$ m^{-3} and 1.4×10^{19} m^{-3} for LH + NB and NB alone, respectively.

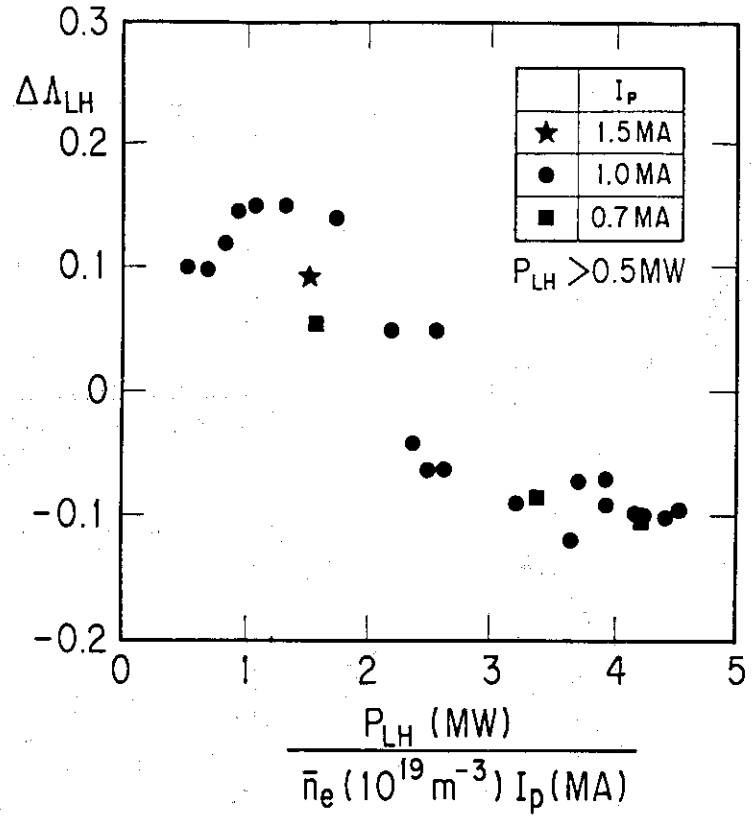

Fig. 8 Dependence of $\Delta\Lambda_{LH}$ defined in eq.(2) on $P_{LH}/\bar{n}_e I_p$.

Appendix Current Profile during LHCD

It is interesting to investigate the transition of current profile during LHCD. For this purpose, we have done the simplified simulation and compare it with the experimental results.

(i) Current Profile Model

We use the cyrindrical coordinate, so that the diffusion equation of the poloidal magnetic field B_p, which can be derived from Maxwell's equation and Ohm's low, is:

$$\frac{\partial B_p}{\partial t} = \frac{\partial}{\partial r}\frac{\eta}{\mu_0}\frac{1}{r}\frac{\partial}{\partial r} r B_p - \frac{\partial}{\partial r}\eta j_{CD} \tag{1}$$

η : Spitzer Resistivity

j_{CD}: noninductive current produced by LHCD

Boundary condition of eq.(1) is:

$$B_p(0) = 0, \quad B_p(a) = \frac{\mu_0 I_p}{2\,a} \tag{2}$$

I_p : total plasma current, which is kept constant

a : plasma minor radius

Then plasma current density j can be obtained from eq.(1).

$$\frac{1}{r}\frac{\partial}{\partial r}(r\,B_p) = \mu_0 j \tag{3}$$

The resistivity of the noninductive current is assumed to be zero so that the electric field is:

$$E = \eta(j - j_{CD}) \tag{4}$$

From the result of eq.(1), plasma internal inductance ℓ_i and one turn voltage V_ℓ can be calculated as follows.

$$\ell_i = \frac{8\pi \int_0^a \frac{B_p^2}{2\mu_0} 2\pi r\, dr}{\mu_0 I_p^2} \tag{5}$$

$$V_\ell = \mu_0 R_p \frac{\dot{\ell}_i}{4} I_p + \frac{2\pi \int_0^a r j^2 2\pi r dr}{I_p} \tag{6}$$

Therefore we can look for the reasonable profile of noninductive current j_{CD} in order to reproduce the trasition of ℓ_i and V_ℓ, which are measured in the experiment.

During LHCD, protile of electron temperature is assumed to be fixed and total plasma current is controlled to be constant without time delay. Noninductive current driven by LHRF is assumed to flow from the beginning of LHCD total of which is 100% of plasma current.

(ii) Comparison of V_ℓ and $\beta_p + \frac{\ell_i}{2}$

The typical experimental result of LHCD is shown in Fig. A1(A). In this case power of LHRF is about 1 MW. After about 200 ms from the start of LHCD, Λ ($= \beta_p + \frac{\ell_i}{2} - 1$) rises to its maximum value ($\Delta\Lambda \simeq 0.05$) and one turn voltage V_ℓ drops to zero. Then Λ decreases slowly at the rate of 0.07/sec. The increase of β_p caused by the formation of electron tail is small ($\Delta\beta_p \simeq 0.01$) as discussed in the section 3, so that the transition of Λ is due to the change of ℓ_i.

In order to reproduce these transition of ℓ_i and V_ℓ, we have seeked for a profile of noninductive current, using the reasonable temperature profile presented in eq.(7).

$$T_e(r) = (T_0 - T_{edge})\{1 - (r/a)^2\}^4 + T_{edge} \tag{7}$$

Finally we have obtained eq.(8) as the noninductive current profile. V_ℓ and ℓ_i calculated from this very simple profile are presented in Fig. A1(b), camparing with the experimental result.

$$j_{CD}(r) = \begin{cases} j_0\{1 - (r/r_B)^2\} & r \le r_B \\ 0 & r_B \le r \le a \end{cases} \tag{8}$$

Transition of V_ℓ and ℓ_i can be explained qualitatively, using the result of simulation as follows. Fig. A2 shows the change of plasma current profile. Before the start of LHCD, the current has peaked profile because of high q(a) ($\simeq 5.2$). When LHCD starts, return current of noninductive current flows in the opposite direction to keep the

magnetic flux. Therefore the negative voltage, caused by this return current is build up and propagates to the plasma surface and center. Resistivity of the plasma surface region is very high, so that this negative voltage propagates more quickly to the plasma surface than to the center. At this time plasma current in the surface region disappears as shown in Fig. A2, so that ℓ_i rises a little. After that ℓ_i decreases slowly. Because current in the central region decreases with long time constant for the sake of low resistivity.

(iii) Discussion

It is found that the transistion of ℓ_i and V_ℓ during LHCD can be explained by very simple model. However, in order to get more physical and quantitative discussion, we have to do more reasonable treatment of the current profile and resistivity under the condition of driving the noninductive current by LHRF.

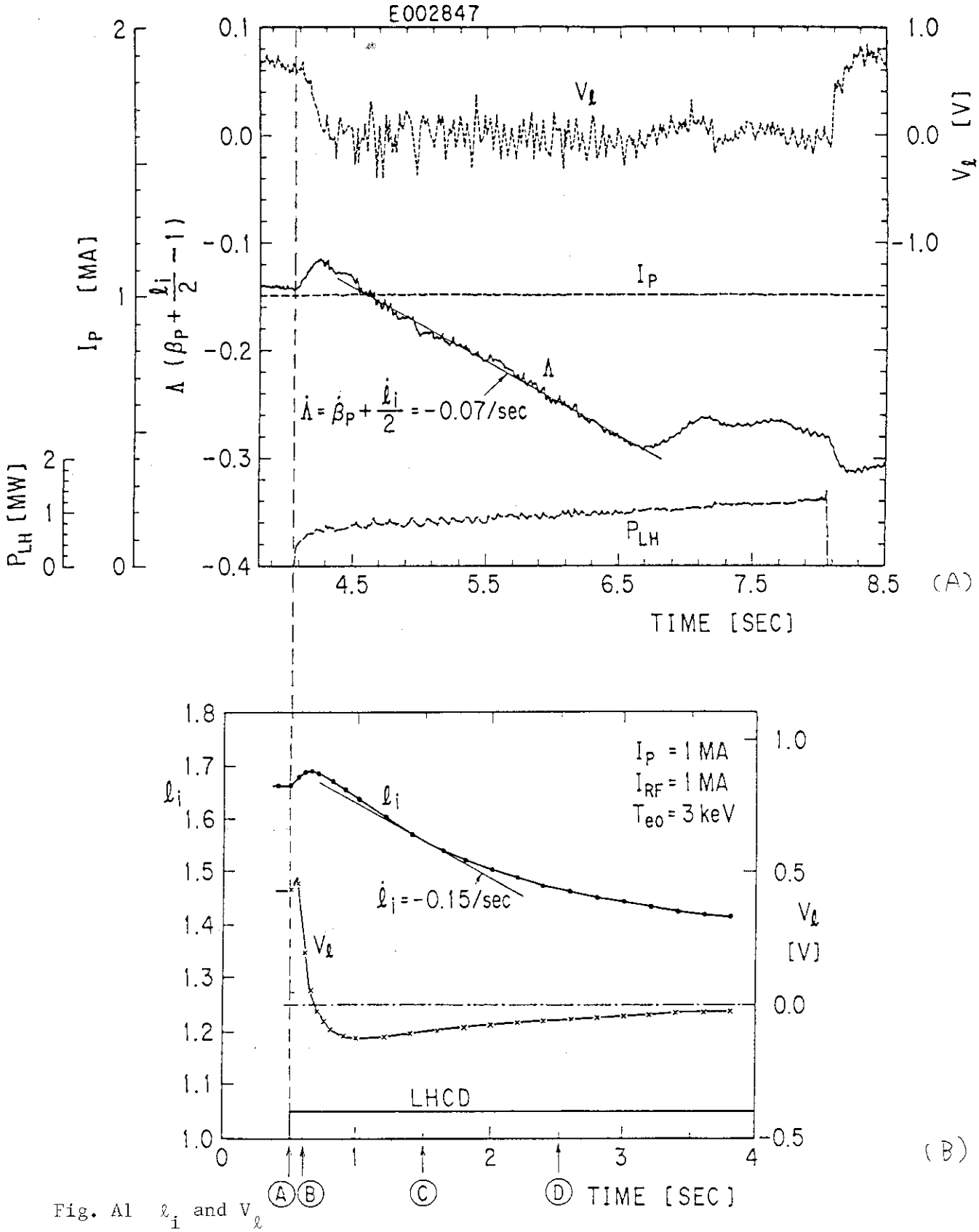

Fig. A1 ℓ_i and V_ℓ
(A) Experiment. (B) Simulation: V_ℓ and ℓ_i show almost the same behavior with (A). ℓ_i decreases at the rate of -0.14/sec ($\dot{\Lambda}$ = -0.07/sec). In this simulation parameters are set as follows. r_B = 0.6 m, T_o = 3 keV, T_{edge} = 200 eV.

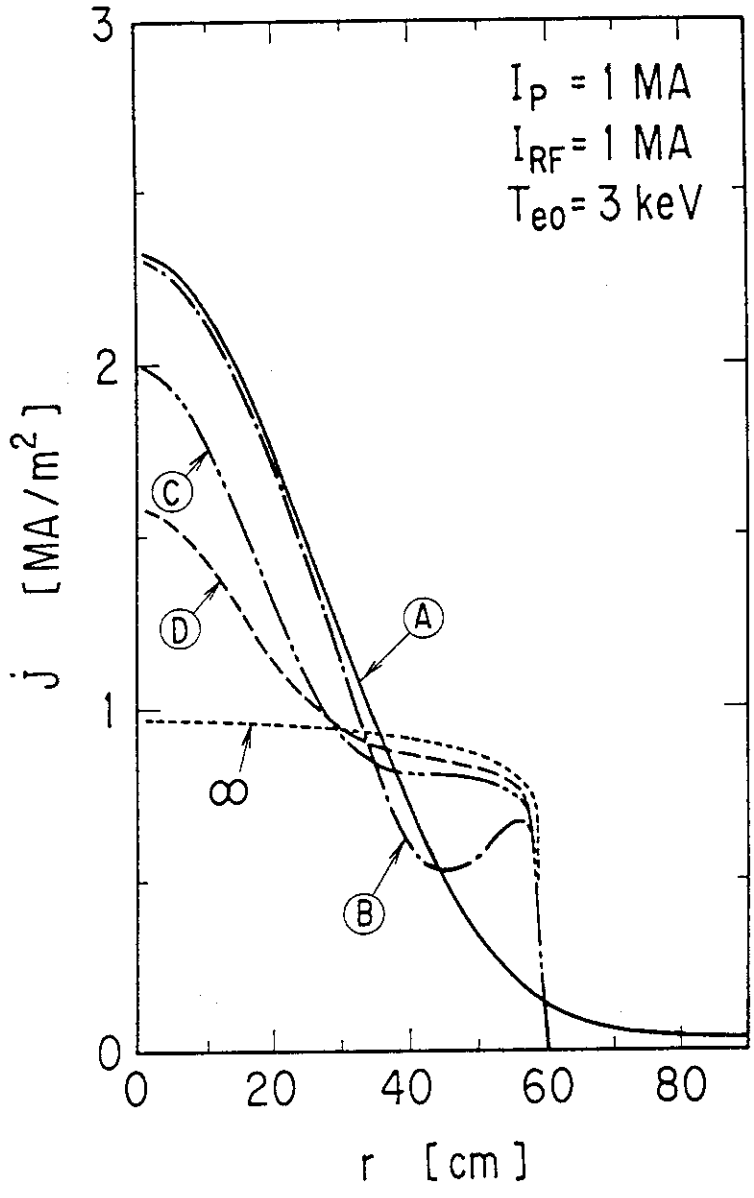

Fig. A2 Transition of Current Profile
Current profile in the case of Fig. A1(B) is presented. Ⓐ is the beginning of the LHCD, after which current profile changes.... Ⓑ 0.1 sec Ⓒ 1 sec Ⓓ 2 sec. ∞ is the profile of the noninductive current $j_{CD}(r)$.